Effect of Pressure on the Fluorescence of Poly[2-methoxy-5-(2′-ethylhexoxy)−*p*-Phenylenevinylene]†

G. Yang, Y. Li, J. O. White, and H. G. Drickamer*

School of Chemical Sciences, Department of Physics and The Frederick Seitz Materials Research Laboratory, University of Illinois, 600 S. Mathews Ave., Urbana, Illinois 61801-3792

Received: December 7, 1998; In Final Form: April 2, 1999

The effect of pressure on both the steady-state intensity and the lifetime of poly[2-methoxy-5-(2′-ethylhexoxy)−*p*-phenylenevinylene] (MEH−PPV) has been measured for the neat polymer and at various dilutions in polystyrene (PS) and poly(methyl methacrylate) (PMMA). At 1 atm the efficiency increases with increasing dilution, especially in PS blends, and new peaks appear in the blends at higher energy. The lower energy peaks decrease in efficiency with pressure. The behavior of the higher energy bands is more complex. The decay rate is very rapid in the neat polymer. In general the decays in the blends are multiexponential. The differences in behavior in PS and PMMA blends can be explained by the greater compatibility of MEH−PPV in PS. In PMMA the MEH−PPV apparently tends to curl up to minimize the area of contact with the medium, leading to dissipation of energy by long-range intramolecular electron transfer.

Introduction

Polymers that fluoresce and may conduct electricity have been widely studied in recent years.[1−3] Among these are a number of derivatives of poly(*p*-phenylenevinylene) (PPV).[4−7] In this paper we present measurements of the fluorescence of poly[2-methoxy-5-(2′-ethylhexoxy)−*p*-phenylenevinylene] (MEH−PPV) as a neat polymer and at various dilutions in polystyrene (PS) and poly(methyl methacrylate) (PMMA) as a function of pressure to ∼65 kbar.

Most publications in this area are in the physics literature, and the analyses are presented using the nomenclature and viewpoint of semiconductor and related physics.[8−13] The literature discusses the excitations in terms of polaron and bipolaron formation and charge transfer although ref 10 assigns emission in benzene solution as $S_1 \rightarrow S_0$ for a different PPV derivative. It is not, however, clear whether this is a charge-transfer emission or whether diffusion of excitation along or between chains is rate-controlling.

In the complex situation in solid polymers neat or in blends the situation is more difficult with the possibilities of intermolecular and long-range intramolecular charge transfer and a variety of possible conformations of both the MEH−PPV and the medium. We feel that for these data only the simplest empirical fit consistent with the complex spectra is justified.

Experiment

Poly[2-methoxy-5-(2′-ethylhexoxy)−*p*-phenylenevinylene] (MEH−PPV) was obtained from Prof. F. Wudl and Dr. R. Helgeson and used without further purification. Poly(methyl methacrylate) (PMMA, medium molecular weight) and polystyrene (PS, average molecular weight of ∼250 000) were purchased from Aldrich. The polymers were used without further purification because none of them gave any emission when irradiated at the excitation laser wavelengths. Spectral grade chloroform was used as the solvent to dissolve MEH−PPV and the polymers.

The thin, pure MEH−PPV film was obtained by spin-coating (∼2500 rpm) from its chloroform solution (0.4 mg/mL) on a thin polyethylene film. MEH−PPV and the polymer (PMMA or PS) were dissolved in chloroform, and the solution was then poured in a glass dish to form a blend film after the solvent evaporation at room temperature. All of the films obtained (pure MEH−PPV film and MEH−PPV in PMMA (or PS) blend samples) were then put in a vacuum oven for a few days at 45 °C. We used a red light in processing the materials.

A transparent film of pure MEH−PPV (about 5 μm in thickness) was obtained, but some of the blend films (about 35 μm in thickness) are different. The lower concentration samples (0.05% in PMMA and 0.2% in PS) are transparent, but the higher concentration samples (0.2% in PMMA and 1% in PS) are slightly foggy. Under the microscope (×50) the lower concentration films are optically clear but tiny red color spots suspended in the film are observed in the higher concentration samples. Apparently, phase separation occurs partially in the higher concentration films.

High pressure is generated in a Merrill-Bassett diamond anvil cell (DAC). The hole diameter of the gasket is about 300 μm. The sample and a tiny ruby chip are placed in the hole, and light mineral oil (Aldrich) is used as a pressure medium. The pressure is determined by the ruby fluorescence shift.[14] The application of the DAC to high-pressure luminescence, absorption, and the time dependence of the emission experiments as well as the experimental setups for these measurements has been described elsewhere.[15−17] For the steady-state emission measurements the excitation is by means of the 441.6 nm line of a He−Cd CW laser. Essentially similar intensity effects are obtained using the 325 nm line of a He−Cd laser. For the measurements of time-dependent decay of the emission the samples are excited by 100 fs pulses from a 76 MHz mode-locked Ti:sapphire laser after frequency-doubling to 405 nm

* To whom correspondence should be sent.

† This work was supported in part by U.S. Department of Energy, Division of Materials Science, Grant DEFG02-96ER45439 through the University of Illinois at Urbana−Champaign, Frederick Seitz Materials Research Laboratory.

10.1021/jp984644t CCC: $18.00
Published on Web 06/06/1999

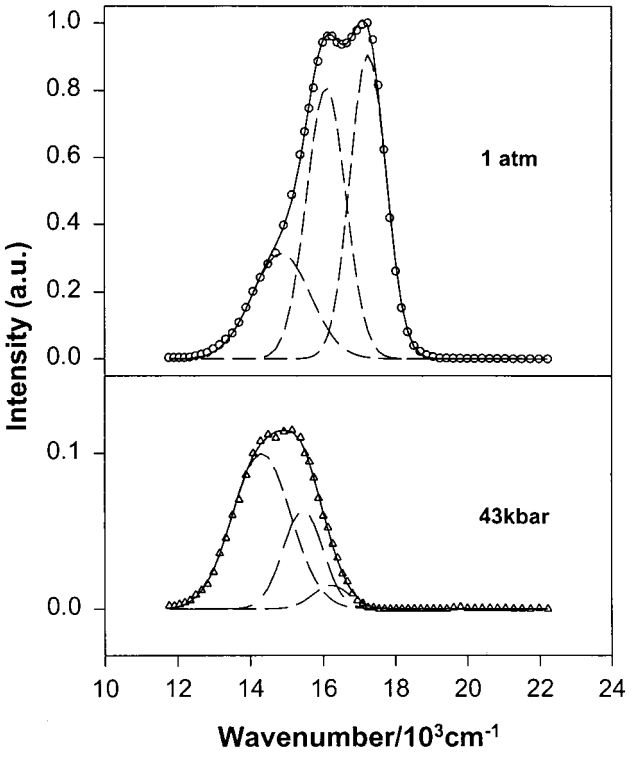

Figure 1. Emission spectra for neat MEH−PPV at 1 atm and 43 kbar with fitting bands: (○, △) experimental data; (- - -) fitting band; (−) sum of fitting bands.

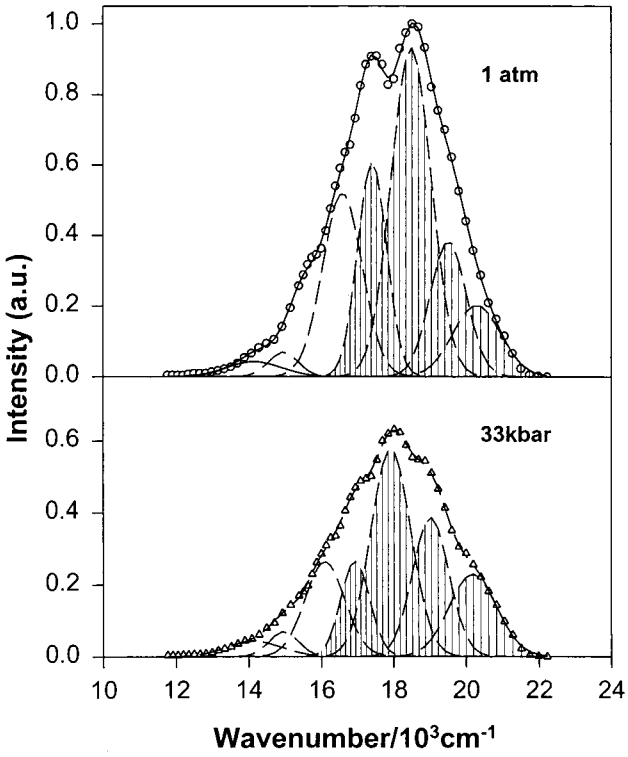

Figure 2. Typical emission spectra for 0.05% blend in PMMA at 1atm and 33 kbar: (○, △) experimental data; (- - -) fitting band; (−) sum of fitting bands.

with a BBO crystal. The detection system involves a Spex 0.27 m monochromator, a Tennelec 863 TAC, an Ortec 582 discriminator, and a Hamatsu R15644 PMT or an MCP-PMT. The system has a basic exponential decay with a time constant of ∼15 ps. However, at an intensity of about 1-100th of the initial value there is a further complex component of about a 100 ps lifetime.

Results

Steady State. In Figure 1 we show typical spectra at two pressures for neat MEH−PPV. They can be fit well with three bands. In the blends, in addition to the three bands that also appear in the neat polymer, a structured emission appears at higher energy that can be accurately fit with four bands. Typical spectra are presented in Figures 2 and 3.

The bands used for fitting the data have half widths at 1 atm of 700−1000 cm^{-1}. These do not change with pressure. The splitting between these subbands is essentially pressure-independent (∼800−1100 cm^{-1}), and except for the three bands in the neat polymer, there are only moderate but definite changes in their relative intensity with pressure. There is no significant broadening or narrowing of the envelope of bands with pressure. In all cases the center of intensity shifts to lower energy by 400−700 cm^{-1} by 35−40 kbar and then shifts back to higher energy by 150−200 cm^{-1} at the highest pressure. These small shifts, plus the fact that they are the same in PS and PMMA, which differ markedly in polarizability, indicate that the excitation is primarily charge transfer with little or no localized (e.g., $\pi-\pi^*$) character. The absorption bands (not shown here) exhibit only modest shifts as well as negligible changes in intensity with pressure either at the maximum absorption or at 441.6 nm.

Since the fitting with three and four bands is accurate and convenient but somewhat arbitrary, for most purposes of discussion we use and compare the intensity effects in two

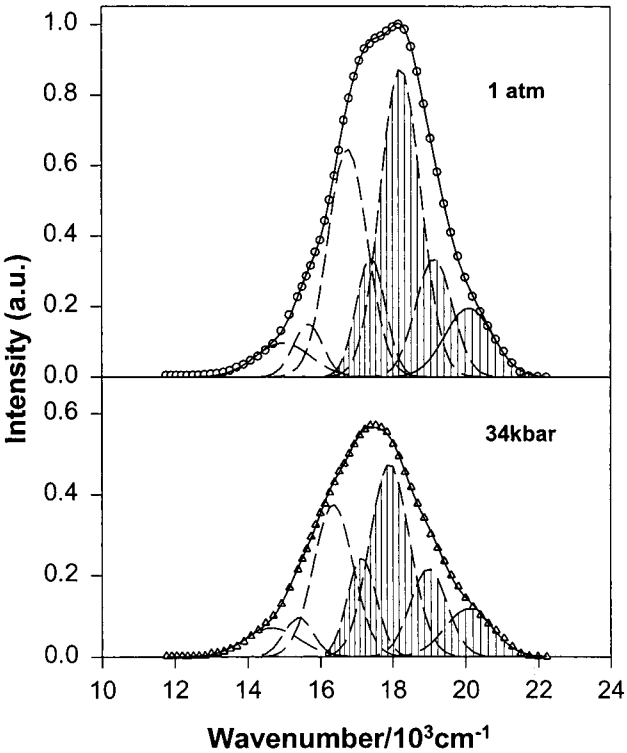

Figure 3. Typical emission spectra for 0.2% blend in PS at 1 atm and 34 kbar: (○, △) experimental data; (- - -) fitting band; (−) sum of fitting bands.

groups: (1) the sum of the areas for the three lower energy bands, which we call the low-energy band (LEB), and (2) the sum of the areas under the four bands that appear only in the blends that we label (HEB). It is a reasonable assumption that the three peaks in the LEB represent the same emissions as

TABLE 1: Relative Emission and Absorption per MEH−PPV Molecule

material	total emission	lower energy emission	higher energy emission
neat MEH−PPV	1	1	
0.2% in PMMA	76	31	45
0.05% in PMMA	170	54	116
1% in PS	36	24	12
0.2% in PS	685	185	500
0.1% in PS	1840	430	1410

Absorption at 441.6 nm per Molecule in the Light Path Normalized to Neat MEH−PPV

neat MEH−PPV	0.05% in PMMA	0.2% in PS	0.1% in PS
1	55	103	136

Relative Efficiency per Photon Absorbed

material	total	LEB
neat MEH−PPV	1.0	1.0
0.05% in PMMA	3.1	1.0
0.2% in PS	6.6	1.8
0.1% in PS	13.5	3.2

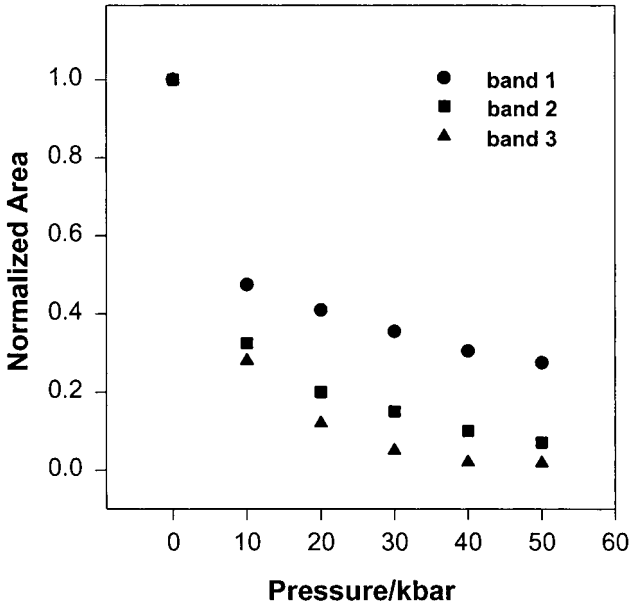

Figure 4. Intensity (normalized to 1 atm value) vs pressure for three bands of neat MEH−PPV.

observed in the neat polymer, but the separation between LEB and HEB is also to a degree arbitrary.

In Table 1 we present the relative emission intensity at 1 atm per molecule in the light path, corrected for concentration and sample thickness. The fitted intensities are grouped as LEB, HEB, and total intensity (LEB + HEB). The total intensity and LEB are normalized to the values obtained for the neat polymer, while the HEB is normalized to the value obtained for the LEB.

In Table 1 we also present, for those samples that exhibit no phase separation, the absorption at 441.6 nm per molecule in the light path, normalized to the value for neat MEH−PPV. The differences among the media are, in significant part, due to differences in the absorption at 441.6 nm relative to that at the absorption maximum. It is also possible that differences in molecular conformation discussed below can change the absorption efficiency. The third item in Table 1 is the relative efficiency per photon absorbed for the total emission and for the LEB.

In Figure 4 we present the change of intensity with pressure for the three bands in the spectrum of the neat polymer. The

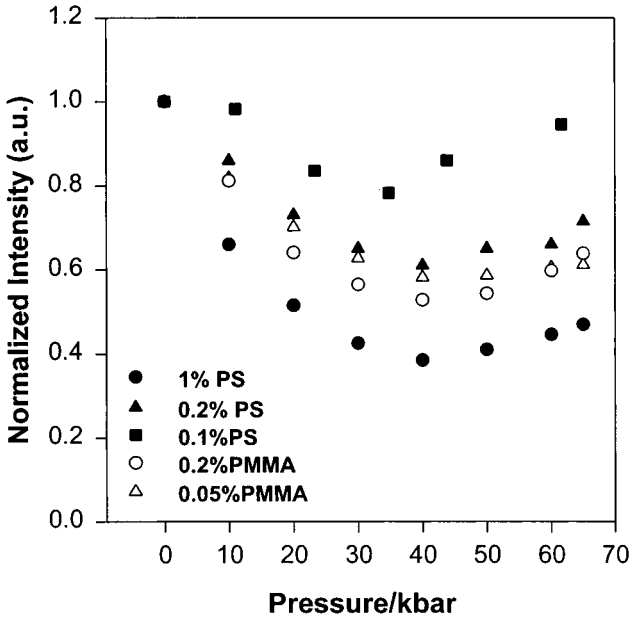

Figure 5. Total emission area vs pressure for 0.2% and 0.05% blends in PMMA and for 1%, 0.2%, and 0.1% blends in PS.

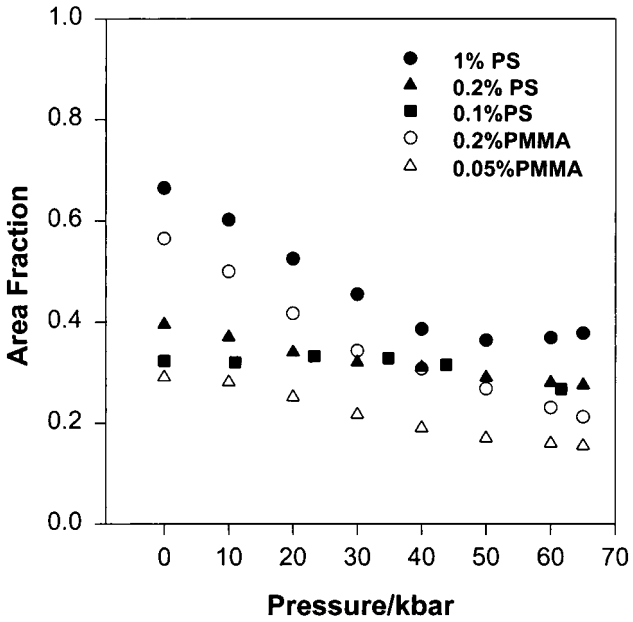

Figure 6. Fraction of LEB relative to the total intensity vs pressure for 0.2% and 0.05% blends in PMMA and for 1%, 0.2%, and 0.1% blends in PS.

two bands that lie at higher energy nearly disappear by 30−40 kbar, while the lowest energy band loses 70−75% of its intensity at 50 kbar.

Figure 5 shows the change in total intensity (HEB plus LEB) with pressure for 0.2% and 0.05% MEH−PPV in PMMA and for 1%, 0.2%, and 0.1% MEH−PPV in PS. In all cases there is a decrease in the first 30 kbar followed by a significant increase. Most of this intensity increase is associated with the HEB.

In Figure 6 we present the change in fraction of LEB relative to the total intensity (LEB/(LEB + HEB)) for all five blends. For the 0.2% MEH−PPV in PMMA and the 1% in PS (the nonuniform samples) the initial fraction is 0.6−0.7, which decreases by a factor of about 2 in 65 kbar. The more dilute samples show an initial fraction of 0.3−0.4 and a modest change with pressure.

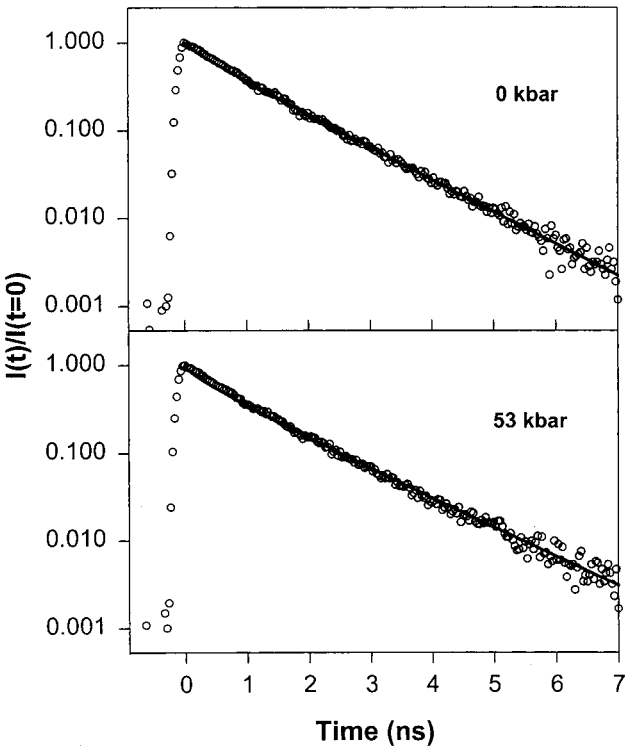

Figure 7. Decay of the 0.2% blend in PS (at 526 nm) at 0 kbar (1atm) and 53 kbar: (○) experimental data; (−) fitting with Förster energy transfer. The double-exponential fit is essentially identical.

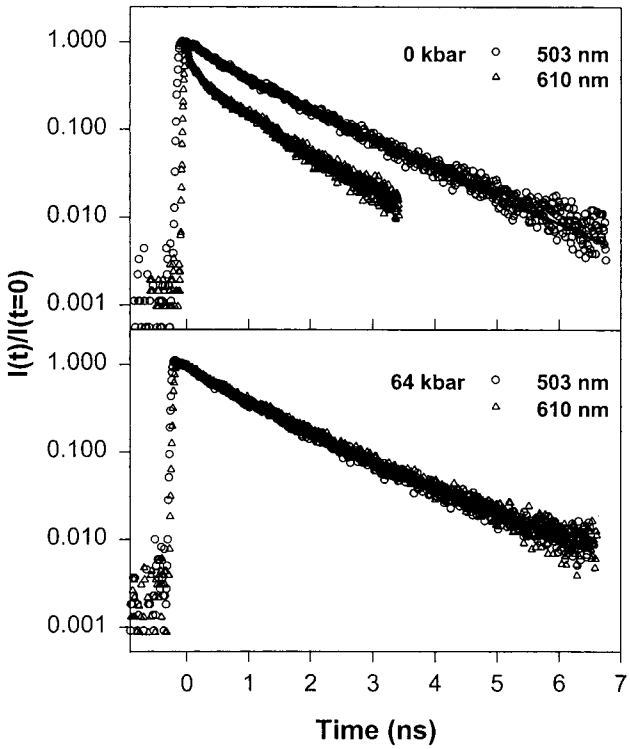

Figure 8. Decay of the 0.05% blend in PMMA (at 503 and 610 nm) at 0 kbar (1 atm) and 64 kbar: (○, △) experimental data; (−) fitting curve (Förster energy transfer for 503 nm at 0 kbar (1 atm) and 64 kbar, three and two exponentials for 610 nm at 1 atm and 64 kbar, respectively. The double-exponential fit at 503 nm is essentially identical with the energy-transfer curve.).

It should be mentioned that each set of data represent the average of two to four loads with very little scatter. All runs, both steady state and time dependent (presented below), were reversible.

Time Dependence. The time dependence of the emission has been measured for the neat MEH−PPV, for the 0.05% blend in PMMA, and for the 0.2% blend in PS.

The measurements were made at two or three different wavelengths. In one case a single exponential decay was observed, but in general, it was necessary to use combinations of two or three exponentials. In all cases the resulting combinations gave very good fits. At any given energy (wavelength) there may be overlap of the fitted peaks, or a given peak may be the combination of several closely spaced emissions.

In a large fraction of the cases it is also possible to get a very good fit for the highest energy emission using the Förster energy transfer theory in the form[18,19]

$$\ln \frac{I}{I_0} = -\left[\frac{t}{\tau_D} + 2\gamma\left(\frac{t}{\tau_D}\right)^{1/2}\right] \quad (1)$$

where τ_D is the donor lifetime. (We treat the highest energy peak as the donor.) γ is a coupling coefficient given by

$$\gamma = \frac{2}{3}\Pi^{3/2} n_A R_0^{\,3} \quad (2)$$

where n_A is the concentration of acceptors and R_0 is the "Förster distance" i.e., the D−A distance such that there is a 50% chance of radiationless energy transfer.

Figures 7 and 8 display typical decay curves for PS and PMMA at one or more emission wavelengths. The line through the data for the higher energy decay represents the fit using Förster energy-transfer theory. The fit using multiple decays is equally good.

TABLE 2: Fluorescence Decay of MEH−PPV in PS and PMMA[a]

		energy transfer fitting		exponential fitting					
		τ/ns	γ	a_1	τ_1/ns	a_2	τ_2/ns	a_3	τ_3/ns
				0.05% in PMMA					
503 nm	1 atm	1.52	0.20	0.47	1.50	0.53	0.80		
	64 kbar	1.92	0.40	0.26	1.90	0.74	0.81		
550 nm	1 atm			0.21	1.62	0.79	0.79		
	64 kbar			0.28	1.75	0.72	0.88		
610 nm	1 atm			0.13	1.49	0.39	0.70	0.48	0.07
	64 kbar			0.28	1.75	0.72	0.88		
				0.2% in PS					
526 nm	1 atm	1.26	0.12	0.64	1.24	0.36	0.75		
	53 kbar	1.46	0.22	0.36	1.46	0.64	0.85		
667 nm	1 atm			1.00	1.10				
	53 kbar			1.00	1.29				

[a] a_1, a_2, a_3: relative amount of the decay curve associated with the corresponding τ. τ: lifetime. γ: defined in the text.

Neat MEH−PPV. By a deconvolution using Fourier transforms, approximate lifetimes of 69 ps at 1 atm and 65 ps at 6 kbar were established.

Blends. In Table 2 we present fits to the time-dependent data at three wavelengths for PMMA and at two wavelengths for PS at 1 atm and at 50−60 kbar. In all cases except PS at 667 nm the decays are multiple exponential.

For PS at 526 nm there are two decays in the nanosecond range differing by a factor of ∼1.6−1.7. Both lifetimes increase by about 15% from 1 atm to the highest measured pressure. The data at 667 nm exhibit a single-exponential decay that increases from 1.10 to 1.29 ns over the pressure range.

For PMMA at 503 nm the longer decay increases from 1.50 to 1.90 ns over the pressure range while decreasing as a fraction of the total from 47% to 26%. The faster decay hardly changes

in the same range of pressure. At 550 nm the two decays are initially 1.62 and 0.79 ns and both increase by ∼10% in 60 kbar. At 610 nm the situation is more complex. At 1 atm it is necessary to use three decays with the fastest one being ∼70 ps. From 15 to 60 kbar the decay pattern is essentially identical to that at 550 nm.

As indicated above, for the highest energy peak (526 nm in PS and 503 nm in PMMA) it is possible to make equally good fits using the Förster energy-transfer model and treating the peak at the highest energy as the donor (see Figures 7 and 8). For PMMA τ_D increases from 1.52 to 1.92 ns from 1 atm to 64 kbar while the coupling coefficient γ essentially doubles in value. For PS τ_D went from 1.26 to 1.46 ns over the pressure range while γ increases by ∼85%.

It should be mentioned that lifetime data were taken and fit at a number of intermediate pressures also. Since they showed continuous progression in the values of the parameters and the overall changes are not in general very large, we present values only for 1 atm and the highest pressure.

Discussion

It is first necessary to consider what is represented by the three-band fit for the neat polymer and the additional four bands used to fit the blends. The bands might represent vibrational splitting, but in materials of this complexity the multiplicity of vibrations should provide a continuum. It is more likely that these bands primarily represent different configurations of the MEH−PPV or different lengths of conjugation over which charge transfer can take place. The number of bands used is the minimum necessary to fit the data, and each band may represent a combination of configurations. Since the overall emission is structured and must be fit by a finite number of subbands, there cannot be a complete continuum of such configurations.

A second point is that the shifts in energy with pressure are moderate in all cases and essentially the same for all media, while there are large effects of pressure on intensity that differ among the media. It appears that the efficiency of emission is not controlled primarily by the radiative and nonradiative rates from the emitting states as predicted by the energy gap law for, for example, $\pi^* \rightarrow$ p emission but by electron-transfer processes and accompanying changes in conformation that are involved in the transfer of excitation from the absorbing state to the emitting state.

A third point to consider is the appearance of the higher energy emission (HEB) in the blends but not in the neat polymer. From the Results we see that the lifetimes associated with the neat polymer are much faster than those for the blends except for the LEB in PMMA at 1 atm. Since the emissions in the neat polymer are heavily quenched by interpolymer electron transfer, it may be that the slower processes represented by the HEB are completely bypassed in that material.

Another possibility of some significance is that the emissions that constitute the HEB arise from conformations of the polymer that can be attained in the blends but not in the neat polymer.

A fourth point involves the difference in behavior of MEH−PPV in PS and in PMMA as illustrated for the steady-state results in Figures 5 and 6 and for the time dependence in Figures 7 and 8, as well as in Table 2. PS is more similar in polarizability to MEH−PPV than PMMA so that there is less tendency for the solute molecules to curl up to expose less surface to the solvent medium and therefore less long-range intrapolymer electron transfer. In addition to differences in these "van der Waals" interactions, these can be differences in geometry and local rigidity between polymeric media and thus different degrees of inhibition of the changes in MEH−PPV conformation that involve electron transfer.

A fifth point is the possibility that in addition to the electron-transfer processes there can be energy transfer between the highest energy peak and the next lower ones utilizing the Förster mechanism. The very good fit of the Förster equation to the high-energy time-dependent data (Figures 7 and 8) makes this a good possibility but not, of course, a certainty. The transfer coefficient γ increases by a factor of 1.7−2.0 in 60 kbar. If there is no change in the character of the acceptor, n_A will increase by ∼1.30−1.35 in 60 kbar because of compression of the medium. Thus, an increase in R_0^3 of 1.30−1.55 is indicated, i.e., an increase of 10−15% in R_0.

Förster's analysis gives three different methods of establishing the efficiency of energy transfer, which have been shown to give equivalent answers. The one that can be applied for our data is

$$E = \pi^{1/2}\gamma \exp(\gamma^2)[1 - \mathrm{erf}(\gamma)] \tag{3}$$

where the error function erf(γ) is given by

$$\mathrm{erf}(\gamma) = 2\pi^{1/2} \int_0^{\gamma} \exp(-x^2)\, dx \tag{4}$$

For both PS and PMMA the increase in efficiency for radiationless energy transfer is a factor of ∼1.45−1.55 from 30 to 60 kbar. However, there is an increase of ∼20% between 0 and 30 kbar while there is an actual decrease in total intensity of the HEB. A possibility is that the increase in Förster transfer is superimposed on effects that cause a continuous decrease in efficiency, which becomes smaller at high pressure, as is exhibited for the LEB.

Neat MEH−PPV. As can be seen from Table 1, at 1 atm the ratio of emission to absorption per molecule in the light path is significantly smaller for the neat polymer than for the blends, especially the PS. The most reasonable explanation of the relatively larger quenching in the neat polymer is electron transfer between chains followed by rapid thermal degradation of the excitation energy. The additional rapid increase in this quenching with pressure shown in Figure 4 must result from the increase in probability of this transfer due to compression. It may be noted that compression is most effective on quenching the highest energy of the three emissions and least effective on the lowest energy peak. In view of the fact that the fitting with three bands is in some degree arbitrary and that the assignment of them is not presently known, it is not profitable to speculate on the causes of this difference.

Blends. The LEB intensity exhibits a substantial initial drop (larger for PMMA than for PS) that levels above 25−30 kbar. The HEB intensity shows a more modest initial drop followed by a significant rise so that the total intensity change is as represented in Figure 5.

The initial drop for both bands may be associated with increased quenching due to long-range intramolecular energy transfer. This effect becomes smaller as the compressibility decreases and the array stiffens at higher pressures.

An explanation for the increase in intensity at higher pressures for the HEB is more tentative. The very small blue shift observed cannot provide for a change via the energy gap law. A plausible scenario is the following. As shown above, the coupling coefficient for Förster energy transfer increases with pressure, at first at a moderate rate and more rapidly above ∼30 kbar. If the donor (D) is a relatively inefficient emitter and the

acceptor (A) is much more efficient, this would give the observed increase in emission intensity.

The above explanation must be regarded as merely a hypothesis, since we have no direct evidence that energy transfer is important except the fit to the highest energy decay curves (Figures 7 and 8). Since the fit of the HEB to four bands is arbitrary, one cannot observe directly the increase in emission of a particular band at the expense of a weak band. The hypothesis is nevertheless reasonable.

Conclusions

The emission properties of neat MEH−PPV and of blends with PS and PMMA show distinct differences. These differences can be qualitatively explained in terms of (1) the minimization of interchain electron transfer in the blends, (2) differences in conformation of MEH−PPV in PS and PMMA, and (3) the possibility of Förster energy transfer with an efficiency increasing with pressure involving the highest energy states observable in the blends but not in the neat polymer.

Acknowledgment. The authors express their very profound gratitude to Professor Fred Wudl and Dr. Roger Helgeson of UCLA for furnishing us with the sample of MEH−PPV. We are also very pleased to acknowledge the continuing support from the U.S. Department of Energy, Division of Materials Science, Grant DEFG 02-96ER45439 through the University of Illinois at Urbana−Champaign Frederick Seitz Materials Research Laboratory. The lifetime studies were performed in the MRL Laser Laboratory.

References and Notes

(1) Tang, C. W.; Vanslyke, S. A. *Appl. Phys. Lett*. **1987**, *51*, 913.

(2) Grem, G.; Leditzky, G.; Ullrich, B.; Leising, G. *Adv. Mater*. **1992**, *4*, 36.

(3) Berggren, M.; Granstrom, M.; Inganas, O.; Anderson, M. *Adv. Mater*. **1995**, *7*, 900.

(4) Wudl, F.; et al. In *Materials for Non-linear Optics: Chemical Perspectives*; American Chemical Society: Washington, DC, 1991.

(5) Buroughes, J. H.; Bradley, D. D. C.; Brown, A. R.; Marks, R. N.; Mackay, K.; Friend, R. H.; Burn, P. L.; Holmes, A. B. *Nature (London)* **1990**, *347*, 539.

(6) Bradley, D. D. C. *Synth. Met*. **1993**, *54*, 401.

(7) Gettinger, C. L.; Heeger, A. J.; Drake, J. M.; Pine, D. J. *J. Chem. Phys.* **1994**, *101*, 1673.

(8) Mizes, H. A.; Conwell, E. W. *Phys. Rev. B* **1994**, *50*, 11243.

(9) Blatchford, J. W.; Jessen, S. W.; Lin, L. B.; Lih, J. J.; Gustafson, T. L.; Epstein, A. J.; Fu, D. K.; Marsella, M. J.; Swager, T. M.; MacDiarmid, A. G.; Yamaguchi, S.; H. Hamaguchi, H. *Phys. Rev. Lett.* **1996**, *76*, 1513.

(10) Gelinck, G. H.; Warman, J. M.; Staring, E. G. J. *J. Phys. Chem*. **1996**, *100*, 5485.

(11) Yan, M.; Rothberg, L. J.; Papadimitrakopoulos, F.; Galvin, M. E.; Miller, T. M. *Phys. Rev. Lett.* **1994**, *72*, 1104.

(12) Yan, M.; Rothberg, L. J.; Kwock, E. W.; Miller, T. M. *Phys. Rev. Lett.* **1995**, *75*, 1992.

(13) Su, W. P.; Schrieffer, J. R.; Heeger, A. J. *Phys. Rev. Lett.* **1979**, *42*, 1698.

(14) Piermarini, G. J.; Block, S. *Rev. Sci. Instrum.* **1975**, *46*, 973.

(15) Jurgensen, C. W.; Drickamer, H. G. *Phys. Rev. B* **1984**, *30*, 7202.

(16) Dreger, Z. A.; Lang, J. M.; Drickamer, H. G. *Chem. Phys. Lett*. **1991**, *185*, 184.

(17) Dreger, Z. A.; Yang, G.; White, J. O.; Li, Y.; Drickamer, H. G. *J. Phys. Chem. A* **1997**, *101*, 9511.

(18) Förster, T. Z. *Ann. Phys. (Leipzig)* **1948**, *55*, 6.

(19) Förster, T. Z. *Faraday Soc. Discussion, Chem. Soc.* **1959**, *27*, 7.